# Comparison of different methods for measuring thermal conductivities

D. Hartung, F. Gather, and P. J. Klar

*I. Physikalisches Institut, Justus-Liebig-Universität Gießen, Heinrich-Buff-Ring 16, 35392 Gießen, Germany*

**Abstract.** Two different methods for the measurement of the thermal conductivity have been applied to a glass (borosilicate) bulk sample. The first method was in the steady-state using an arrangement of gold wires on the sample to create a thermal gradient and to measure the temperatures locally. This allows one to calculate the in-plane thermal conductivity of the sample. The same wire arrangement was also used for a $3\omega$-measurement of the direction-independent bulk thermal conductivity. The $3\omega$-approach is based on periodical heating and a frequency dependent analysis of the temperature response. The results of both methods are in good agreement with each other for this isotropic material, if thermal and radiative losses are accounted for. Our results demonstrate that especially in the case of thin-film measurements, finite element analysis has to be applied to correct for heat losses due to geometry and radiation. In this fashion, the wire positions can be optimized in order to minimize measurement errors.

**Keywords:** Thermal conductivity measurement, $3\omega$-method, glass
**PACS:** 65.60.+a, 66.70.+w, 68.60.-p

## I. INTRODUCTION

The determination of the thermal conductivity of materials is important for the optimization of their thermoelectric figure of merit. The measurement of bulk materials is well understood, whereas for thin films the measurement methods are more complex and a simple transfer of bulk methods is usually not possible. Currently, different approaches for the determination of the thermal properties in cross-plane and in in-plane direction of thin films are being developed and tested. Many methods for the in-plane thermal conductivity measurement are steady-state methods of various designs or methods based on a van-der-Pauw approach. Methods for investigating the cross-plane thermal conductivity are the $3\omega$-method and the derivate time-domain thermoreflectance method.

The main principle of the steady-state methods is the establishment of a constant heat flow in the sample. The analysis is typically based on measurements of local temperatures at defined distances from the heat source [1, 2, 3, 4, 5, 6, 7]. Depending on the chosen geometry cross-plane and in-plane thermal conductivity can be determined. However usually heat losses are unavoidable due to the finite geometry of the heater and sensor arrangement.

The principle of the $3\omega$-method and time-domain thermoreflectance differs from that of the steady-state methods. A dynamical approach is used where the sample is perturbed by periodical heating either by an electric current or by laser radiation. The analysis of the response signal as a function of modulation frequency yields the thermal conductivity [8, 9, 10]. As these are perturbative approaches, radiation losses are minimal. These methods are mainly established for cross-plane thermal conductivity measurements and usually yield only little or uncertain information about in-plane properties.

The van-der-Pauw method is applicable only for measuring the in-plane thermal conductivity of isotropic thin films. Resistors are located at the four corners of the thin film which serve at the same time as temperature sensors and heaters. A heat current is injected at one corner and extracted from the neighboring right corner. The temperature difference of the two opposite corners is measured. Afterwards the same procedure is carried out with the neighbor on the left. The thermal conductivity is determined by combining the results of both measurements [11, 12, 13].

Here, we compare steady-state in-plane measurements of the thermal conductivity of an isotropic bulk glass sample with corresponding $3\omega$-measurements.

## II. METHOD

The principle of the steady-state in-plane thermal conductivity measurement is illustrated in Figure 1. The broad wire on the top of the borosilicate glass test structure serves as the heating-wire. The other three wires are temperature sensors. All the wires are operated in four terminal sensing. To heat the sample a DC-current is applied to the broad wire. For an infinite wire in an ideal two-dimensional plane, the Joule heat causes a heat flux in one dimension (to the right and to the left) from the middle of the wire to the sensor wires located parallel to

*9th European Conference on Thermoelectrics*
AIP Conf. Proc. 1449, 381-384 (2012); doi: 10.1063/1.4731576

the heater. In the steady-state the temperature gradient is constant and perpendicular to the wires. The three sensor wires located at defined distances $x_i$ from the heater are used to determine the local temperature $T_i$. For this purpose a calibration curve (resistance versus temperature) needs to be determined for each sensor wire. From the temperature values determined for any pair of heaters $i$ and $j$, the thermal conductivity $\kappa$ of the sample can be derived as [14, 15]:

$$\kappa = -q\frac{x_i - x_j}{2(T_i - T_j)} \tag{1}$$

where $q = P/A$ is the heatflux which is equal to the power $P$ divided by the cross-section $A = L \cdot d$, where $L$ is the length of the heater and $d$ the sample thickness. The factor of 2 in the denominator of Eq. 1 accounts for equal heat flows to the left and to the right of the heater wire.

In the experiment, this ideal situation may only be approximated because of the finite thickness of the specimen and the finite lengths of heater and sensor wires. Furthermore heat losses due to radiation and along the contact metallization cannot be avoided. The length of the heater wire needs to be long compared to the distance of the sensor wires from the heater ($L > x_i$) and the sample should be thin ($d < x_i$) to approximate the ideal situation. The specimen is coupled to heat sinks located on the left and on the right at a large distance from the wire arrangement.

The specimen holder is attached to a heating block, which is fixed on a nitrogen reservoir. A copper box encloses the specimen holder to minimize radiation effects. This assembly is mounted in a vacuum chamber. The measurement parameters are computer controlled.

The same set-up is used for the $3\omega$-measurements where the sensor wires were used for the measurement [8, 9]. In this case the whole backside of the sample is in contact with a copper heat sink.

## III. SAMPLE FABRICATION

The used borosilicate glass has the dimensions of 1.4 cm×1.8 cm×50 µm. A thin glass is necessary for a good approximation of the 2D-measurement situation. The wire arrangement is defined on the sample by photolithography followed by a metallization and a lift-off step. The metallization consists of a 5 - 8 nm thick chromium layer which serves as a primer and 100 - 110 nm silver layer used as the actual wire material. Figure 2 shows an optical image of the fabricated arrangement of the silver wires. The heater wire and the sensor wires are basically located in between four crosses. The horizontal bars on the left and on the right serve as heat sinks. Each of the thin sensor wires is connected to four contact pads.

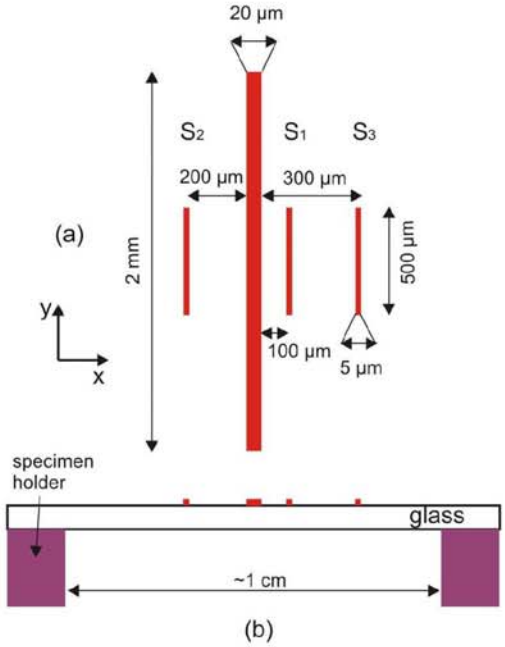


**FIGURE 1.** (a) Schematic illustration of the top surface of the wire arrangement. The heater wire is located in the middle of the illustration. The three other wires ($S_1$, $S_2$, $S_3$) are sensing wires located at different distances from the heater wire. (b) Corresponding cross section of a borosilicate test structure with the wire arrangement on it.

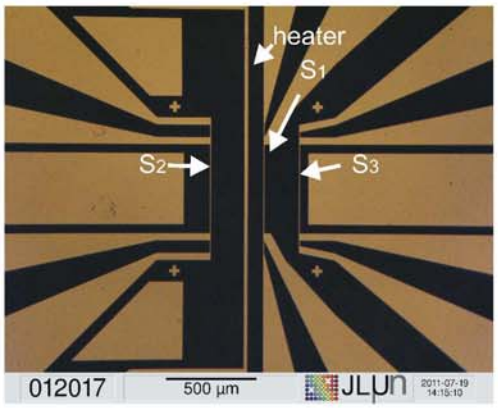


**FIGURE 2.** Optical image of the top surface of the wire arrangement made of metall on 50 µm thick borosilicate glass.

## IV. RESULTS

The results of the temperature-dependent measurements from 240 K to 320 K by the steady-state approach and the $3\omega$-method are shown in Figure 3. The solid line with the star symbols depicts the results of the $3\omega$-measurements.

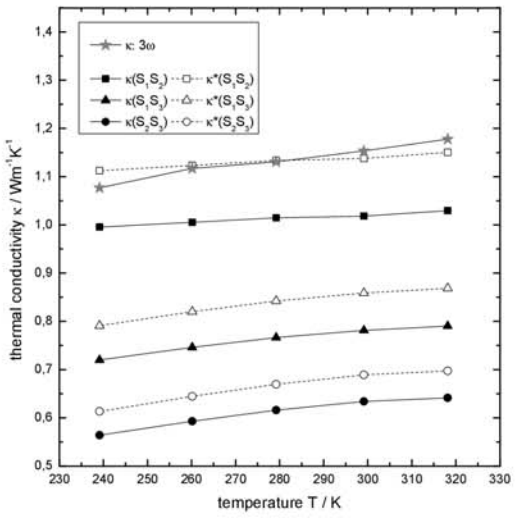


**FIGURE 3.** Thermal conductivity $\kappa$ of a 50 μm borosilicate glass measured with the $3\omega$ and a steady-state method. The three sensor configurations are corrected to $\kappa^*$.

The values of $\kappa$ obtained by the $3\omega$-method are increasing with increasing temperature are typical for glass [16]. The three solid curves with the black symbols denote the results of the steady-state measurements derived using Eq. 1 for the three combinations of sensor pairs ($S_1S_2$), ($S_1S_3$), and ($S_2S_3$). The thermal conductivities obtained by the steady-state method for all three pairs of sensors are lower than those of the $3\omega$-measurement. Furthermore the results for the three sensor pairs show a clear trend. With increasing mean distance of the sensor pair from the heater wire, i.e. 150 nm for ($S_1S_2$), 200 nm for ($S_1S_3$), and 250 nm ($S_2S_3$), the thermal conductivity derived using the equation for the idealized situation decreases. The reasons are heat losses parallel to the wire direction and radiation losses perpendicular to the sample plane which become more important with increasing distance from the heater. These are not accounted for in Eq. 1 where the heat flow only takes place in $x$-direction, i.e. in-plane and perpendicular to the wires. To estimate the heat losses due to finite geometry, we performed a finite element calculations using the software package *Ansys*. In the model the sample is ideally 2-dimensional with the heater wire embedded in the sample plane. The sensor wires and contacts have been neglected. The temperature distribution about the heater wire due to the finite length of the heater is shown in Figure 4. The isotherms are no longer parallel to the heater wire as expected. The reduction of the temperature at the positions of the sensor wires has been estimated by taking corresponding temperatures along a line perpendicular to the heater, which crosses the heater wire at its center. The curves of the temperature decrease as a function of position $x$ for the ideal case (1D-model) and for the finite element model (2D-model) are plotted in Figure 5. The two curves deviate with increasing $x$ due to the heat losses. The effect can be empirically accounted for by modifying Eq. 1 using a scaling factor $\alpha_{ij}$

**TABLE 1.** Correction factors $\alpha_{ij}$ accounting for heat losses due to finite geometry of the wire arrangement.

| **Correction** | $\alpha_{12}$ | $\alpha_{13}$ | $\alpha_{23}$ |
|---|---|---|---|
| Value | 0.895 | 0.91 | 0.92 |

$$\kappa^* = -q\frac{x_i - x_j}{2(T_i - T_j)\cdot\alpha_{ij}} \tag{2}$$

where $\alpha_{ij} = \frac{\Delta T_{1D}}{\Delta T_{2D}}$ with $\Delta T_{1D}$ and $\Delta T_{2D}$ denoting the temperature differences between the positions $x_i$ and $x_j$ in the two models. The values derived for the sensor pairs are given in Table 1. Applying Eq. 2 to the experimental data yields the corrected values of the steady-state measurements. These are plotted as the three dotted curves with the open symbols in Figure 3 for all sensor pairs. After this correction the data for the sensor pairs ($S_1S_2$), whose mean distance from the heater is smallest, are in good agreement with the $3\omega$-results. The results for the two other sensor pairs are still smaller than those of the $3\omega$-measurement and still show a decrease with increasing mean distance from the heater. These findings suggest that radiation losses are no longer negligible at larger mean distances of the sensor wires from the heater. The radiation losses are difficult to estimate as they not only depend on the specimen and its thermal coupling to the heat sink, but also on the absolute temperatures of the heater, the heat sink, and the surrounding shielding.

## V. CONCLUSIONS

We measured the thermal conductivity of an isotropic borosilicate glass sample by a steady-state method and by the $3\omega$-method using the same wire arrangement on the sample surface. An agreement between results obtained by the two methods can be obtained when correcting the steady-state measurements for heat losses, as long as radiation losses are negligible. The latter is only the case if the sensor wires are located close to the heater. The results on this isotropic sample demonstrate that steady-state approaches are prone to errors. These errors can only be minimized by a careful design of sensor and heater wires accompanied by theoretical modeling using finite element techniques. A verification is partic-

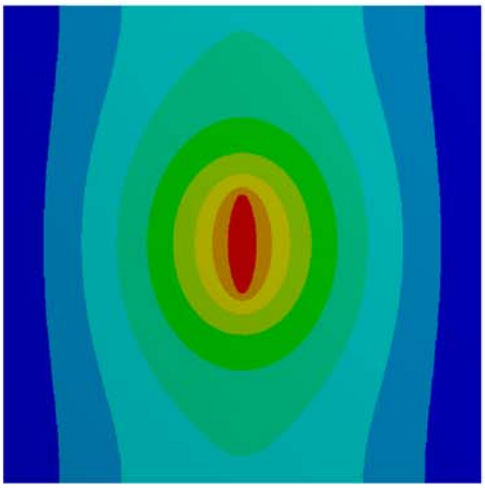

**FIGURE 4.** A picture of the 2D simulation for the 2mm long heater wire by the software *Ansys* shows the 2D heat flow.

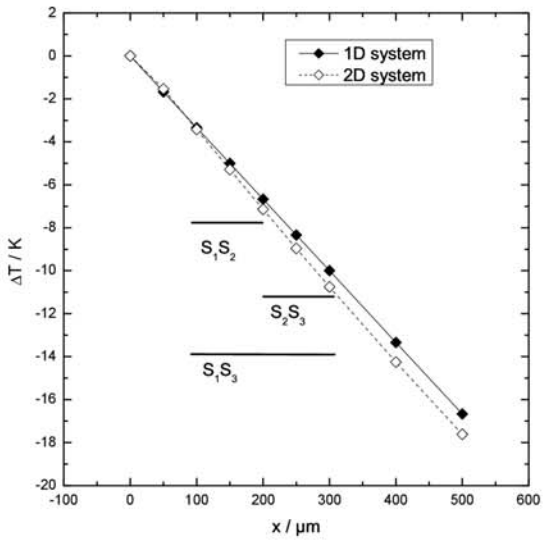


**FIGURE 5.** Development of the temperature decrease $\Delta T$ versus the distance from the heater wire for the ideal 1D case and the 2D case corresponding to a finite wire.

ularly difficult in the case of anisotropic samples where a comparison with established methods such as the $3\omega$-method is not possible.

## ACKNOWLEDGMENTS

We are grateful for funding by the DFG in the framework of the priority program SPP1386 "nanostructured thermoelectric materials".

## REFERENCES

1. A. McConnell, S. Uma, and K. Goodson, *Microelectromechanical Systems, Journal of Microelectromechanical Systems* **10**, 360–369 (2001).
2. F. Völklein, *Thin Solid Films* **188**, 27–33 (1990).
3. F. Völklein, and E. Kessler, *physica status solidi (a)* **81**, 585–596 (1984).
4. M. Kleiner, S. Kuhn, and W. Weber, "Thermal conductivity of thin silicon dioxide films in integrated circuits," in *Solid State Device Research Conference, 1995. ESSDERC'95. Proceedings of the 25th European*, IEEE, 1995, pp. 473–476.
5. F. Brotzen, P. Loos, and D. Brady, *Thin Solid Films* **207**, 197–201 (1992).
6. M. von Arx, O. Paul, and H. Baltes, *Microelectromechanical Systems, Journal of Microelectromechanical Systems* **9**, 136–145 (2000).
7. F. Volklein, and H. Balles, *Microelectromechanical Systems, Journal of Microelectromechanical Systems* **1**, 193–196 (1992).
8. B. Yang, J. Liu, K. Wang, and G. Chen, *Applied physics letters* **80**, 1758 (2002).
9. D. Cahill, *Review of Scientific Instruments* **61**, 802–808 (1990).
10. D. Cahill, W. Ford, K. Goodson, G. Mahan, A. Majumdar, H. Maris, R. Merlin, and S. Phillpot, *Journal of Applied Physics* **93**, 793 (2003).
11. S. Hafizovic, and O. Paul, *Sensors and Actuators A: Physical* **97**, 246–252 (2002).
12. O. Paul, P. Ruther, L. Plattner, and H. Baltes, *Semiconductor Manufacturing, IEEE Transactions on* **13**, 159–166 (2000).
13. L. J. van der PAUW, *Philips Res. Repts* **13** (1958).
14. X. Zhang, and C. Grigoropoulos, *Review of scientific instruments* **66**, 1115–1120 (1995).
15. A. Irace, and P. Sarro, *Sensors and Actuators A: Physical* **76**, 323–328 (1999).
16. C. Kittel, *Physical Review* **75**, 972 (1949).